Dovepress

ORIGINAL RESEARCH

Curcumin-Modified Selenium Nanoparticles Improve S180 Tumour Therapy in Mice by Regulating the Gut Microbiota and Chemotherapy

Rong Zhang [ID]*, Wenjuan Zhang [ID]*, Qiuhua Zhang [ID]*, Lijun Wang, Fengzhu Yang, Wenlong Sun, Zhengbao Xu, Chao Wang, Xinhua Song, Meng Wang

School of Life Science and Medicine, Shandong University of Technology, Zibo, 255000, People's Republic of China

*These authors contributed equally to this work

Correspondence: Meng Wang, Email wm902012@163.com

Purpose: This study aimed to synthesize curcumin-modified selenium (Cur/Se) nanoparticles via a simple and green method for tumour treatment and explore their effects on the gut microbiota.

Methods: Curcumin was applied as a reducing and capping agent for the construction of Cur/Se nanoparticles with Tween 80 as a stabilizer. The drug release behaviour and DPPH and ABTS radical scavenging activities of the Cur/Se nanoparticles were detected. MTT and CCK8 assays were used to evaluate the cytotoxicity against HeLa and S180 tumour cells. The cellular distribution, uptake and reactive oxygen species (ROS) levels were detected. In vivo anti-S180 tumour activity was studied by oral administration. 16S rRNA Illumina high-throughput sequencing technology was used to analyse the gut microbiota in ileocecal faeces.

Results: Nanoparticles with good water dispersibility and a size of 6.86 nm were obtained. The characteristic peaks of curcumin were observed in the UV and FTIR spectra of the Cur/Se nanoparticles. Curcumin release from the Cur/Se nanoparticles occurred in a pH-dependent and sustained manner at 48 h. The Cur/Se nanoparticles presented significantly higher DPPH and ABTS radical scavenging rates than the same concentration of free curcumin. At 48 h, the Cur/Se nanoparticles showed higher cytotoxicity against HeLa and S180 tumour cells. The results of the cellular uptake experiments revealed that the Cur/Se nanoparticles significantly delivered more curcumin into the HeLa tumour cells and induced greater ROS production. In vivo, the Cur/Se nanoparticles significantly inhibited S180 tumours, with a 54.33% tumour inhibitory rate. Cur and Cur/Se nanoparticles significantly reduced the relative abundances of *Rikenellaceae_RC9_gut_group, Enterorhabdus* and *Bilophila* and increased the relative abundance of *Lachnospiraceae_UCG-006*. Moreover, Cur/Se nanoparticle treatment significantly improved the relative abundance of *Limosilactobacillus* compared with that in the curcumin group.

Conclusion: Cur/Se nanoparticles could increase the bioactivity of curcumin and improve cancer therapy by regulating the gut microbiota.

Keywords: curcumin, nanodelivery system, chemotherapy, ROS, gut microbiota

Introduction

Current studies have shown that gut microbiota dysbiosis is associated with the regulation of the occurrence and development of various tumours, such as colorectal cancer,[1] breast cancer[2] and hepatocellular carcinoma.[3] Changes in gut microbiota diversity may have carcinogenic effects, and a reduction in gut microbiota diversity significantly reduces the immune function of patients with tumours.[4] Many microbial metabolites have significant impacts on anticancer immunity.[5] Moreover, the gut microbiota plays an important role in the metabolism of chemotherapy drugs, which affects antitumour efficacy.[6] Therefore, a deeper exploration of the effects of chemotherapy on the gut microbiota could provide feasible solutions for antitumour treatment.

In recent years, curcumin has made progress in the treatment of tumours. One of the main antitumour mechanisms of curcumin is to promote apoptosis by regulating reactive oxygen species.[7,8] Recent studies have shown that curcumin has a positive effect on the gut microbiota. Curcumin plays a role in preventing and combating cancer by increasing the abundance of beneficial microbes and decreasing the abundance of pathogenic microbes.[9,10] However, curcumin is insoluble in water. The bioavailability of curcumin is very poor, making it difficult to exert its curative effect.[11] Therefore, improving the solubility of curcumin is an urgent problem to be solved.

Currently, nanotechnology is a promising strategy for drug delivery and cancer treatment.[12,13] Nanocarriers have unique advantages in improving drug delivery, bioavailability and targeting. Research has shown that nanocarriers can overcome the hydrophobicity of curcumin.[14,15] Nanoselenium has attracted widespread attention because of its high biocompatibility, surface modification ability and low toxicity.[16] However, nanoselenium is usually unstable and tends to aggregate into inactive black precipitates. Therefore, developing new methods to improve the stability of nanoselenium has become the focus of current research. Chemical methods are among the main methods used to prepare selenium nanoparticles. Chemical synthesis methods often consume many chemical reagents and have high costs and high toxicity. The use of plant-based nanoselenium provides a strategy to solve these problems.

Considering that curcumin has excellent reducing properties, it can be used as a reducing and capping agent in the preparation of nanoselenium. To obtain well-dispersed curcumin-modified selenium (Cur/Se) nanoparticles, Tween 80 was added as a stabilizer. In this study, Cur/Se nanoparticles were successfully prepared via a one-step method with excellent water dispersion. The physicochemical and biological properties were studied. The antitumour activity of the Cur/Se nanoparticles was evaluated in vitro and in vivo. This study preliminarily investigated the antitumour mechanism of nanoparticles. 16S rRNA Illumina high-throughput sequencing technology was used to investigate the effects of Cur/Se nanoparticles on the gut microbiota. This study provides strategies through which nanoparticles exert antitumour effects by regulating the gut microbiota.

Materials and Methods

Materials

Curcumin (Cur), 2.2-diphenyl-1-picrylhydrazyl (DPPH), 2.2'-azino-bis(3-ethylbenzothiazoline-6-sulfonic acid) diammonium salt (ABTS) and potassium persulfate ($K_2S_2O_8$) were purchased from Shanghai Macklin Biochemical Co., Ltd. (Shanghai, China). Sodium selenite, Tween 80, salicylic acid, iron (II) sulfate heptahydrate and hydrogen peroxide were purchased from Sinopharm Chemical Reagent Co., Ltd. (Shanghai, China). CCK-8 reagent was purchased from Beyotime Biotechnology, Inc. (Shanghai, China). 3-(4,5-Dimethylthiazol-2-yl)-2,5-diphenyltetrazolium bromide (MTT) was purchased from Sigma Aldrich China Inc. (Shanghai, China).

Synthesis and Characterization of Cur/Se Nanoparticles

Cur was dissolved in dimethyl sulfoxide solution. Sodium selenite was dissolved in a Tween 80 aqueous solution. The solutions were subsequently mixed and stirred for 3 h at room temperature. The products were transferred into a dialysis bag and dialyzed against distilled water for 2 d (MWCO = 1000 Da). The obtained Cur/Se nanoparticles were characterized via UV-Vis spectrophotometry (Hitachi UV-3310, Japan), transmission electron microscopy (TEM; Thermo Fisher FEI Talos F200x, USA), dynamic light scattering (Malvern NANO-ZS, UK), inductively coupled plasma–mass spectrometry (ICP–MS; Thermo Fisher ICAP–Qc, USA), and Fourier transform infrared spectroscopy (FTIR, Nicolet 5700, USA).

Cur Release

The drug release behaviour of Cur and Cur/Se nanoparticles was detected at pH 7.4 and 5.5 at 37 °C via a previously described method with some modifications.[17] The same concentrations of free Cur and Cur/Se nanoparticle solutions were placed in a dialysis bag (MWCO = 1000 Da), immersed in phosphate buffer solution (PBS, pH 7.4 and 5.5) containing 0.1% Tween 80, and shaken (100 rpm) at 37 °C. The samples were collected, and the release media were

supplemented at specified time points. The Cur concentration of the samples was detected via a UV-Vis spectrophotometer.[18,19]

DPPH Radical Scavenging Activity Assay

The DPPH radical scavenging capacity of the samples was determined via a previously described method with some modifications.[20] Briefly, DPPH ethanol solution (0.1mM, 2 mL) was mixed with the same drug concentration of Cur or Cur/Se NPs solution (2 mL) and incubated at room temperature in the dark for 30 min. Then, the absorbance of the reaction mixture was measured at 517 nm.

ABTS Radical Scavenging Activity Assay

The ABTS radical scavenging capacity of the samples was determined via a previously described method with some modifications.[21] Briefly, the same amounts of ABTS (7.4 mmol/L) and $K_2S_2O_8$ (2.6 mmol/L) were mixed at room temperature and reacted in the dark for 16 h. Then, the mixture was diluted to obtain an absorbance of 0.70 at 734 nm. The diluted ABTS reagent (3 mL) was mixed with different sample solutions (1 mL) and incubated at room temperature in the dark for 20 min. The absorbance of the reaction mixture was measured at 734 nm.

The following Formula (1) was used to calculate the DPPH and ABTS radical scavenging activities of Cur and Cur/Se NPs.

$$Scavenging\ activity = \left[1 - \frac{A_1 - A_2}{A_0}\right] \times 100\% \tag{1}$$

where A_0 and A_1 are the absorbance of the DPPH or ABTS radical solution without and with Cur or Cur/Se NPs solution, respectively, and A_2 is the absorbance of the Cur or Cur/Se NPs samples.

Antitumour Activity of Cur/Se Nanoparticles in vitro

The human cervical cancer cell line HeLa and the mouse sarcoma S180 tumour cell line S180 and the human hepatocyte cell line L02 were purchased from ATCC, and the cells were cultured with DMEM. The cytotoxicity of Cur/Se nanoparticles to HeLa tumour cells was detected via the MTT assay. HeLa tumour cells at the logarithmic growth stage were digested with trypsin, and culture medium was added to prepare a cell suspension. The cells were subsequently seeded into 96-well plates in 100 μL of culture medium and cultured overnight. Cur and Cur/Se nanoparticle solutions were prepared with the same concentration gradient of Cur (0.5 μg/mL, 5 μg/mL, 25 μg/mL, 50 μg/mL, 100 μg/mL, and 250 μg/mL). The cells were cultured with 25 μL of the above solutions for 24 h or 48 h. Then, 31.5 μL of MTT solution (5 mg/mL, in PBS) was added to each well and incubated for another 4 h. Afterward, the culture medium was removed, and 200 μL of DMSO was added. The absorbance of each well was detected by using a microplate reader at 570 nm. The cytotoxicity of Cur/Se nanoparticles to L02 cells was detected via the MTT assay as mentioned above.

The cytotoxicity of the Cur/Se nanoparticles to S180 tumour cells was detected via a CCK-8 assay. S180 tumour cell suspensions were prepared and seeded into 96-well plates in 80 μL of culture medium. Culture medium without S180 tumour cells was used as a blank control. Cur and Cur/Se nanoparticle solutions were prepared with the same concentration gradient of Cur (0.5 μg/mL, 5 μg/mL, 25 μg/mL, 50 μg/mL, 100 μg/mL, and 250 μg/mL). The cells were cultured with 20 μL of the above solutions for 24 h or 48 h. Then, 10 μL of CCK-8 solution was added to each well and incubated for another 4 h. The absorbance of each well was detected by using a microplate reader at 450 nm.

Intracellular Distribution of Cur/Se Nanoparticles

A suspension of HeLa tumour cells was prepared via the above method and seeded into a 6-well plate at a density of 2×10^5/mL. After incubation for 24 h, the tumour cells were cocultured with Cur or Cur/Se nanoparticle solutions (Cur, 2 μg/mL) for predetermined durations. After washing with PBS three times, the fluorescence was observed by a fluorescence microscope (Nikon ECLIPSE Ti-S, Japan).

Cellular Uptake of Cur/Se Nanoparticles

A suspension of HeLa tumour cells was prepared via the above method and seeded into a 12-well plate at a density of 1×10^5/mL. After incubation for 24 h, the tumour cells were cocultured with Cur or Cur/Se nanoparticle solutions (Cur, 2 μg/ mL) for predetermined durations. After being washed with PBS three times, the cells were collected and resuspended in PBS for fluorescence analysis via flow cytometry (BD Accuri™ C6 Plus, USA). At least 1×10^4 cells were analysed via flow cytometry for each sample.

Intracellular Reactive Oxygen Species (ROS) Detection

Intracellular ROS generation was detected via 2′,7′-dichlorofluorescein-diacetate (DCFH-DA). HeLa cells were cocultured with Cur or Cur/Se nanoparticle solutions (Cur, 2 μg/mL) in 12-well plates for 4 h. The cells were washed with PBS and incubated in DCFH-DA working solution (10 μM, 1 mL per well) at 37 °C in the dark for 30 min. Then, the cells were washed with PBS three times. The cells were collected and resuspended in PBS for analysis of intracellular ROS via flow cytometry. At least 1×10^4 cells were analysed via flow cytometry for each sample.

In vitro Antibacterial Study

Bacterial suspensions at logarithmic growth stage with OD = 0.5 were diluted 100 times. The bacterial suspensions were subsequently seeded into 96-well plates in 80 μL of culture medium. Cur and Cur/Se nanoparticle solutions were prepared at the same concentration gradient of curcumin (0.5 μg/mL, 5 μg/mL, 25 μg/mL, 125 μg/mL, 250 μg/mL, and 500 μg/mL). The bacteria were cultured with 20 μL of the above solutions for 17 h. The absorbance of each well was detected by using a microplate reader at 600 nm.

Antitumour Activity of Cur/Se Nanoparticles in vivo

An ICR male mouse was intraperitoneally inoculated with 1.0×10^6 S180 cells. On Day 7, S180 ascites were extracted under aseptic conditions and diluted 1:3 with aseptic saline. Five-week-old ICR male mice were inoculated with 0.1 mL of tumour cell suspension subcutaneously in the right axillary area. Therefore, S180 tumour-bearing ICR mouse models were constructed. When the tumour volume increased to 50–100 mm^3, the S180 tumour-bearing mice were randomly divided into 3 groups: the control group, Cur group and Cur/Se nanoparticle group (n = 6). The antitumour experiment was carried out according to previous methods with some modifications.[18] Cur and Cur/Se nanoparticle solutions were orally administered daily at a dose of 10 mg/kg Cur for 10 days. Body weight and tumour volume were measured every two days. At the end of treatment, the tumours were harvested and weighed. The heart, liver, spleen, lung and kidney were collected for haematoxylin and eosin (HE) staining. After the mice were killed, the abdominal cavity was opened quickly, and the intestinal tissue was removed. The faecal matter in the ileocecum of each mouse was rapidly collected and stored in a 1.5 mL sterile EP tube at −80 °C. 16S rRNA sequencing was used to analyse the structural composition and diversity of the gut microbiota.

Statistical Analysis

Statistical analysis was performed via Microsoft Excel software and GraphPad Prism software. All the experiments were repeated at least three times. After confirming that the values followed a normal distribution, a two-tailed Student's t-test was applied to determine the significant differences. The data are presented as the means ± standard errors, and $p < 0.05$ was considered statistically significant.

The 16S rRNA sequencing work of the gut microbiota was completed in cooperation with Shanghai Majorbio Biopharm Technology Co., Ltd. (Shanghai, China). The data were analysed on the online platform of the Majorbio Cloud Platform. The experimental results are presented as the means ± standard errors, and $p < 0.05$ was considered statistically significant.

Results

Synthesis and Characterization of Cur/Se Nanoparticles

The detail of the synthesis of Cur/Se nanoparticles is shown in Scheme 1. The Cur/Se nanoparticles were prepared by reducing sodium selenite with curcumin in one step. Curcumin was applied as a reducing and capping agent, and Tween 80 was used as a stabilizer. A diagram of the preparation of Cur/Se nanoparticles is shown in Figure 1a. An orange–red aqueous solution of Cur/Se nanoparticles was obtained, as shown in Figure 1a. The Cur/Se nanoparticles showed good water dispersion. A total of 25 mL of Cur/Se nanoparticle solution was prepared, and the curcumin concentration of the Cur/Se nanoparticles was 350 μg/mL. The ICP–MS results revealed that the Se concentration was 1.6 μg/mL.

A TEM image of the nanoparticles is shown in Figure 1b. The morphology of the nanoparticles was nearly spherical with a regular shape and a diameter of 5–10 nm. The Cur/Se nanoparticles clearly exhibited lattice fringes, and the selected area of the electron diffraction results revealed that the nanoparticles had a polycrystalline structure. The hydrodynamic size of the Cur/Se nanoparticles was 6.86 nm, as detected by dynamic light scattering (Figure 1c), which was in accordance with the TEM results.

The UV-Vis spectra of the Cur and Cur/Se nanoparticles presented characteristic maximum absorption peaks at 432 nm with no redshift or blueshift phenomenon (Figure 1d). The nanometreization of Cur does not affect its UV-Vis absorption.

The FTIR spectra of the Cur and Cur/Se nanoparticles are shown in Figure 1e. The characteristic absorption peaks at 3514 cm^{-1}, 1628 cm^{-1}, and 1153 cm^{-1} corresponded to the stretching vibrations of the phenolic hydroxyl group, mixed C=O and C=C, and C-O-C of Cur, respectively. The bending vibration of C=C (1600 cm^{-1}) and out-of-plane deformation vibration (856 and 744 cm^{-1}) of the benzene ring were observed in the FTIR spectrum of Cur. These characteristic absorption peaks were observed in the FTIR spectrum of the Cur/Se nanoparticles. The results showed that the structure of curcumin in the Cur/Se nanoparticles did not obviously change. The Cur/Se nanoparticles presented the same characteristic peaks as the mixture of curcumin and Tween 80. Owing to the low content of selenium, the FTIR spectra did not reveal interactions between curcumin and nanoselenium. The stability of the Cur/Se nanoparticles was dependent mainly on physical interactions with Tween 80.

Cur Release

The release behaviour of the samples at different pH values is shown in Figure 2a and b. Within 72 h, the amount of drug released from free Cur was approximately 56% at pH 7.4. The amount of drug released from the Cur/Se nanoparticles was approximately 49%. As the pH decreased to 5.5, the amount of drug released from free Cur or Cur/Se nanoparticles increased to approximately 96% and 66%, respectively. The drug release rate of the Cur/Se nanoparticles was slower than that of free Cur, which showed sustained release behaviour. The pH of the release medium could affect the release behaviour of Cur from the samples. At pH 5.5, both the free Cur and Cur/Se nanoparticles resulted in faster drug release
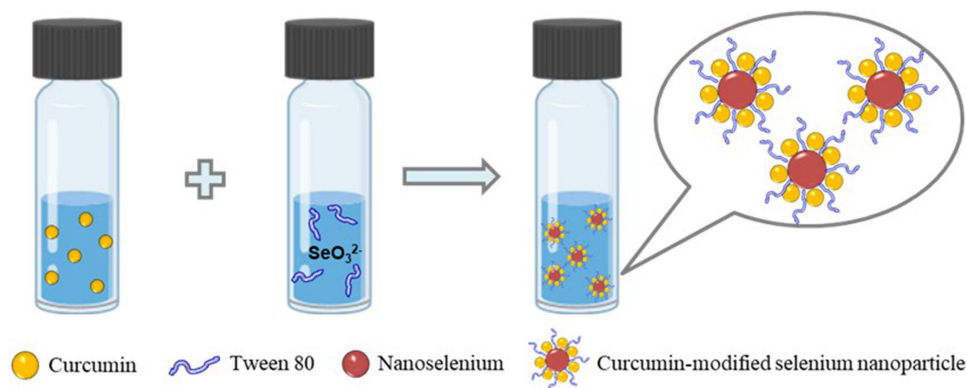
Scheme 1 Schematic illustration of the curcumin-modified selenium nanoparticle preparation. Curcumin is a reducing and capping agent. Tween 80 is a stabilizer, and sodium selenite is the selenium source.
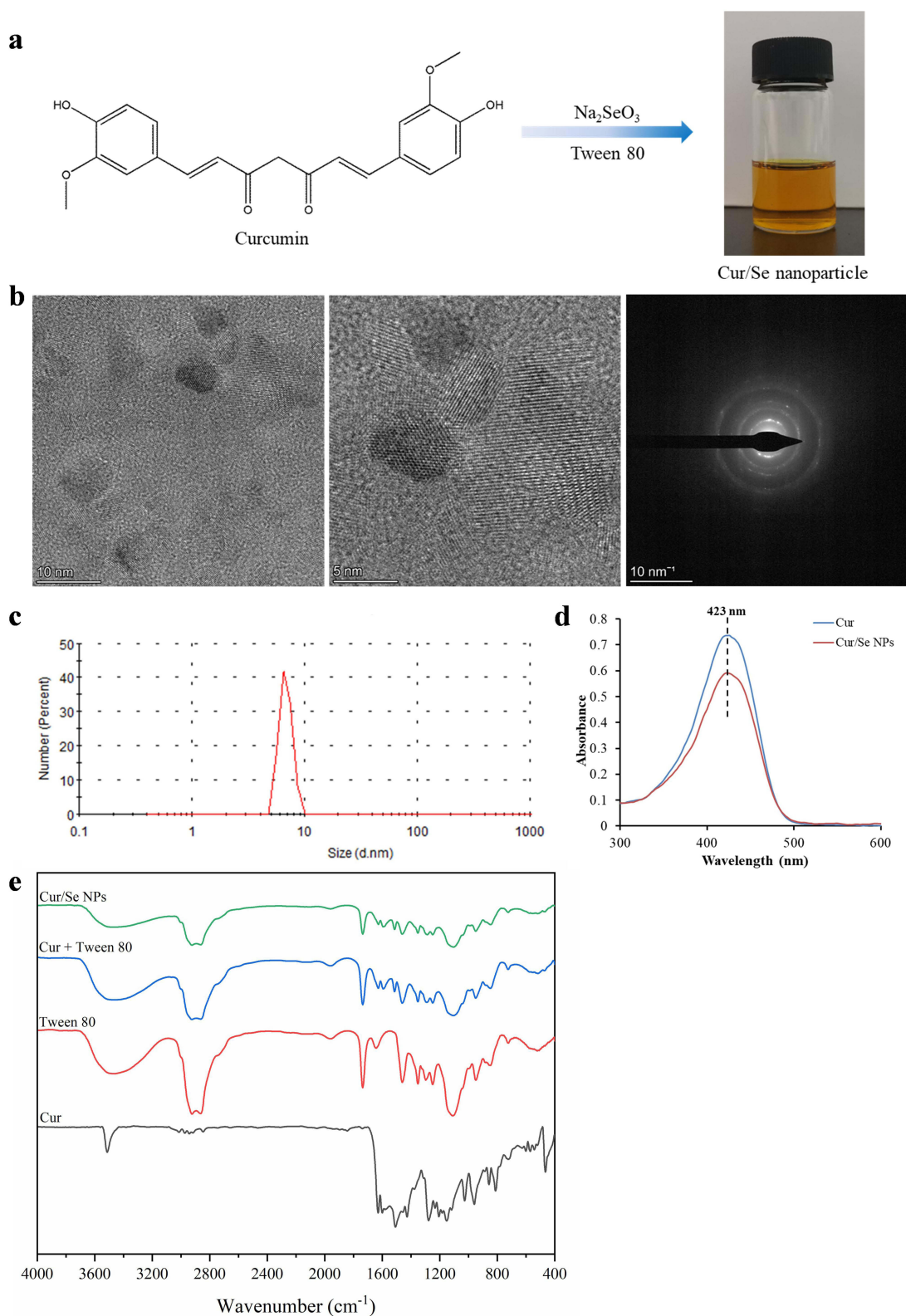
Figure 1 Preparation and characterization of Cur/Se nanoparticles. (**a**) Preparation of Cur/Se nanoparticles. (**b**) TEM image of Cur/Se nanoparticles. (**c**) Hydrodynamic diameters of Cur/Se nanoparticles detected by dynamic light scattering. (**d**) UV-Vis spectra of Cur and Cur/Se nanoparticles. (**e**) FTIR spectra of Cur, Tween 80, the mixture of curcumin and Tween 80 (Cur + Tween 80), and Cur/Se nanoparticles.
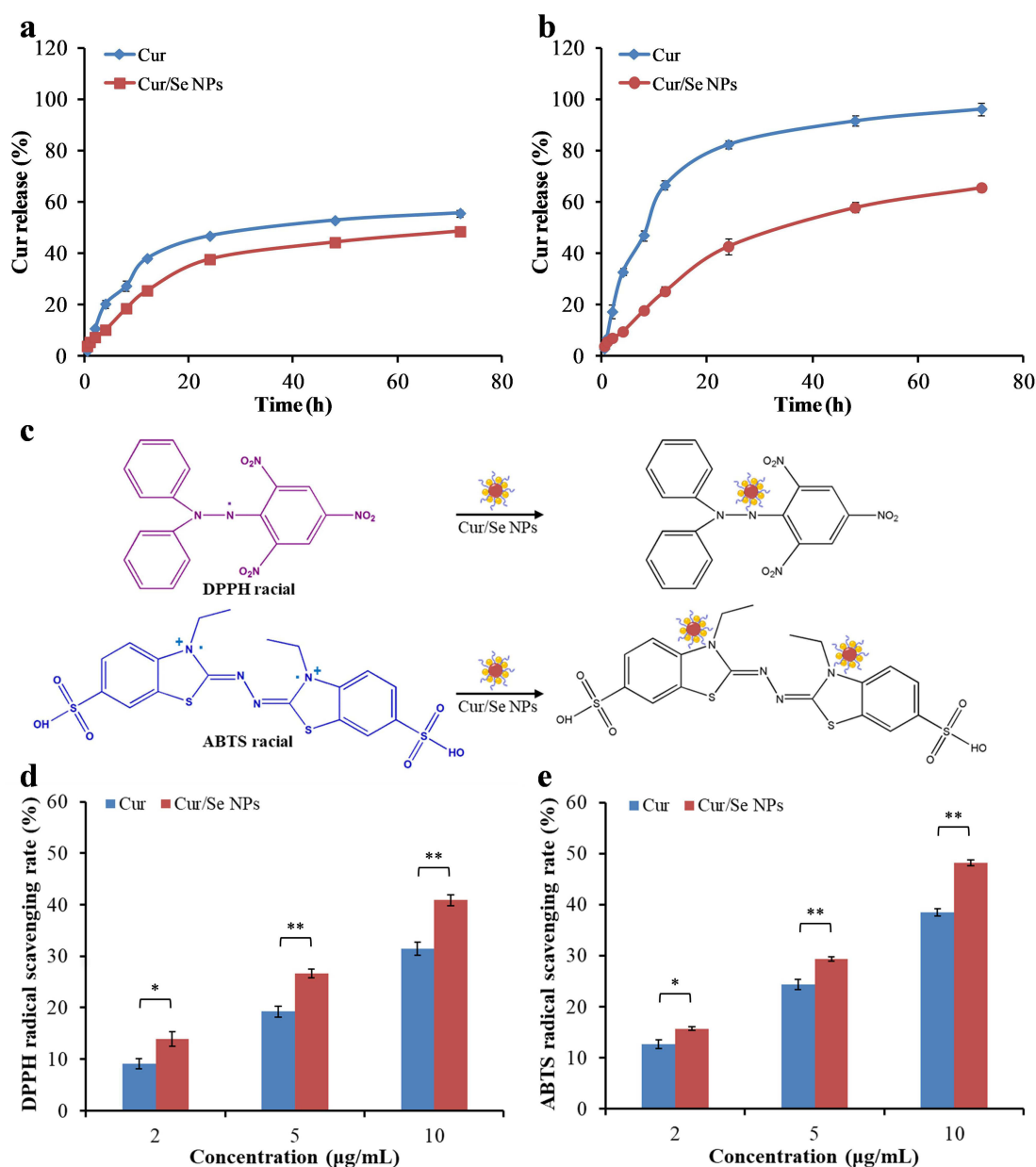
Figure 2 Drug release behaviour of Cur and Cur/Se nanoparticles at (**a**) pH 7.4 and (**b**) pH 5.5. (**c**) Schematic illustration of the DPPH and ABTS radical scavenging process. (**d**) DPPH radical scavenging rates of curcumin and Cur/Se nanoparticles. (**e**) ABTS radical scavenging rates of curcumin and Cur/Se nanoparticles. The results are expressed as the means ± SDs (n = 3). **$P < 0.01$. *$P < 0.05$.

than at pH 7.4. The formation of Cur/Se nanoparticles did not affect the pH-sensitive release behaviour of curcumin. These results implied that the drug release behaviour from Cur/Se nanoparticles occurred in a pH-dependent and sustained manner.

Antioxidant Activities

DPPH and ABTS radicals are widely used to test the antioxidant activity of antioxidant substances. Both Cur and selenium are reported to possess antioxidant activity. Thus the antioxidant ability of Cur/Se nanoparticles was tested via DPPH and ABTS reagents (Figure 2c). The DPPH radical scavenging rates of Cur and Cur/Se nanoparticles are shown in Figure 2d. The DPPH radical scavenging rates of curcumin at concentrations of 2 µg/mL, 5 µg/mL and 10 µg/mL were 9.1 ± 1.0%, 19.2 ± 1.1% and 31.4 ± 1.2%, respectively. For the same concentration of Cur/Se nanoparticles, the DPPH

radical scavenging rates were 13.9 ± 1.4%, 26.6 ± 0.9% and 40.9 ± 1.0%, respectively. Both Cur and Cur/Se nanoparticles exhibited concentration-dependent DPPH radical scavenging activity. The DPPH radical scavenging activity was significantly improved for the formation of Cur/Se nanoparticles. The results of the ABTS radical scavenging rates of Cur and Cur/Se nanoparticles were similar to those of DPPH (Figure 2e). The ABTS radical scavenging rates of curcumin at concentrations of 2 μg/mL, 5 μg/mL and 10 μg/mL were 12.7 ± 0.9%, 24.3 ± 1.0% and 38.4 ± 0.7%, respectively. For the same concentration of Cur/Se nanoparticles, the DPPH radical scavenging rates were 15.6 ± 0.4%, 29.3 ± 0.4% and 48.2 ± 0.6%, respectively. An increase in the curcumin concentration of Cur and Cur/ Se nanoparticles was beneficial for antioxidant activity. The Cur/Se nanoparticles significantly increased the ABTS radical scavenging rates. These results implied that Cur/Se nanoparticles had better antioxidant activity than Cur.

Cell Viability Assay

The antitumour activities of free Cur and Cur/Se nanoparticles were detected in HeLa and S180 tumour cells, and the IC$_{50}$ values were calculated via GraphPad Prism software. The cytotoxicity of Cur and Cur/Se nanoparticles to HeLa tumour cells at 24 h is shown in Figure 3a. The Cur/Se nanoparticles showed significant cytotoxicity at a curcumin concentration of 5 μg/mL. Free Cur did not effectively inhibit the growth of HeLa tumour cells. As the concentration of free Cur increased to 50 μg/mL, the viability of HeLa tumour cells was as high as 51.1% ± 1.8%. The viability of the HeLa tumour cells significantly decreased to 13.5% ± 1.4% after treatment with the Cur/Se nanoparticles. The IC$_{50}$ value of the Cur/Se nanoparticles was 10.4 μg/mL against HeLa tumour cells at 24 h. As the incubation time increased to 48 h, the cytotoxicity of the free Cur and Cur/Se nanoparticles increased (Figure 3b). The IC$_{50}$ values of Cur and Cur/Se nanoparticles were 15.7 μg/mL and 4.7 μg/mL, respectively, against HeLa tumour cells at 48 h. The cytotoxicity of Cur and Cur/Se nanoparticles to S180 tumour cells is shown in Figure 3c and d. Free Cur showed no obvious cytotoxicity, with 78.2% ± 4.3% cell viability at the highest concentration of 50 μg/mL at 24 h (Figure 3c). For the Cur/Se nanoparticles, the viability of the S180 tumour cells significantly decreased to 3.8% ± 4.1%. The IC$_{50}$ value of the Cur/Se nanoparticles was 26.7 μg/mL against the S180 tumour cells at 24 h. As the incubation time increased to 48 h, the cytotoxicity of the free Cur and Cur/Se nanoparticles also increased (Figure 3d). The IC$_{50}$ values of Cur and Cur/Se nanoparticles were 33.0 μg/mL and 8.4 μg/mL, respectively, against S180 tumour cells at 48 h. These results implied that Cur and Cur/Se nanoparticles exhibited concentration- and time-dependent cytotoxicity. Compared with free Cur, the Cur/Se nanoparticles had a stronger effect on killing tumour cells at the same concentration and duration of treatment.

The cytotoxicity of Cur and Cur/Se nanoparticles to L02 cells was also detected. At a concentration of 50 μg/mL, the viability of L02 cells was 56.9% ± 3.7% and 14.8% ± 1.4% after treatment with Cur and Cur/Se nanoparticles, respectively, for 24 h (Figure 3e). The IC$_{50}$ value of the Cur/Se nanoparticles was 25.6 μg/mL against L02 cells at 24 h. As the incubation time increased to 48 h, the cytotoxicity of the free Cur and Cur/Se nanoparticles increased (Figure 3f). The IC$_{50}$ values of Cur and Cur/Se nanoparticles were 10.5 μg/mL and 11.2 μg/mL, respectively, against L02 cells at 48 h. These results implied that the Cur and Cur/Se nanoparticles were also cytotoxic to normal cells.

Intracellular Distribution and Uptake of Cur/Se Nanoparticles

The cellular distributions of free Cur and Cur/Se nanoparticles were detected via fluorescence microscopy (Figure 4a). The fluorescence images revealed that both Cur and Cur/Se nanoparticles rapidly entered the tumour cells at 1 h. Cur and Cur/Se nanoparticles were observed in whole tumour cells, mainly in the cytoplasm. The cellular uptake of free Cur and Cur/Se nanoparticles was subsequently quantified via flow cytometry (Figure 4b). At 1 h, the relative fluorescence intensities of the Cur and Cur/Se nanoparticles were 1.30 ± 0.06 and 1.93 ± 0.02 times greater than that of the control, respectively. As the incubation time increased to 4 h, the relative fluorescence intensity of the Cur and Cur/Se nanoparticles significantly increased to 2.23 ± 0.01 and 2.42 ± 0.06 times that of the control, respectively. The intracellular accumulation of Cur and Cur/Se nanoparticles was time dependent. More curcumin was delivered into the HeLa tumour cells by the Cur/Se nanoparticles than free Cur at the same time points of 1 h and 4 h. These results indicated that the Cur/Se nanoparticles improved the accumulation of intracellular curcumin to increase its cytotoxicity.
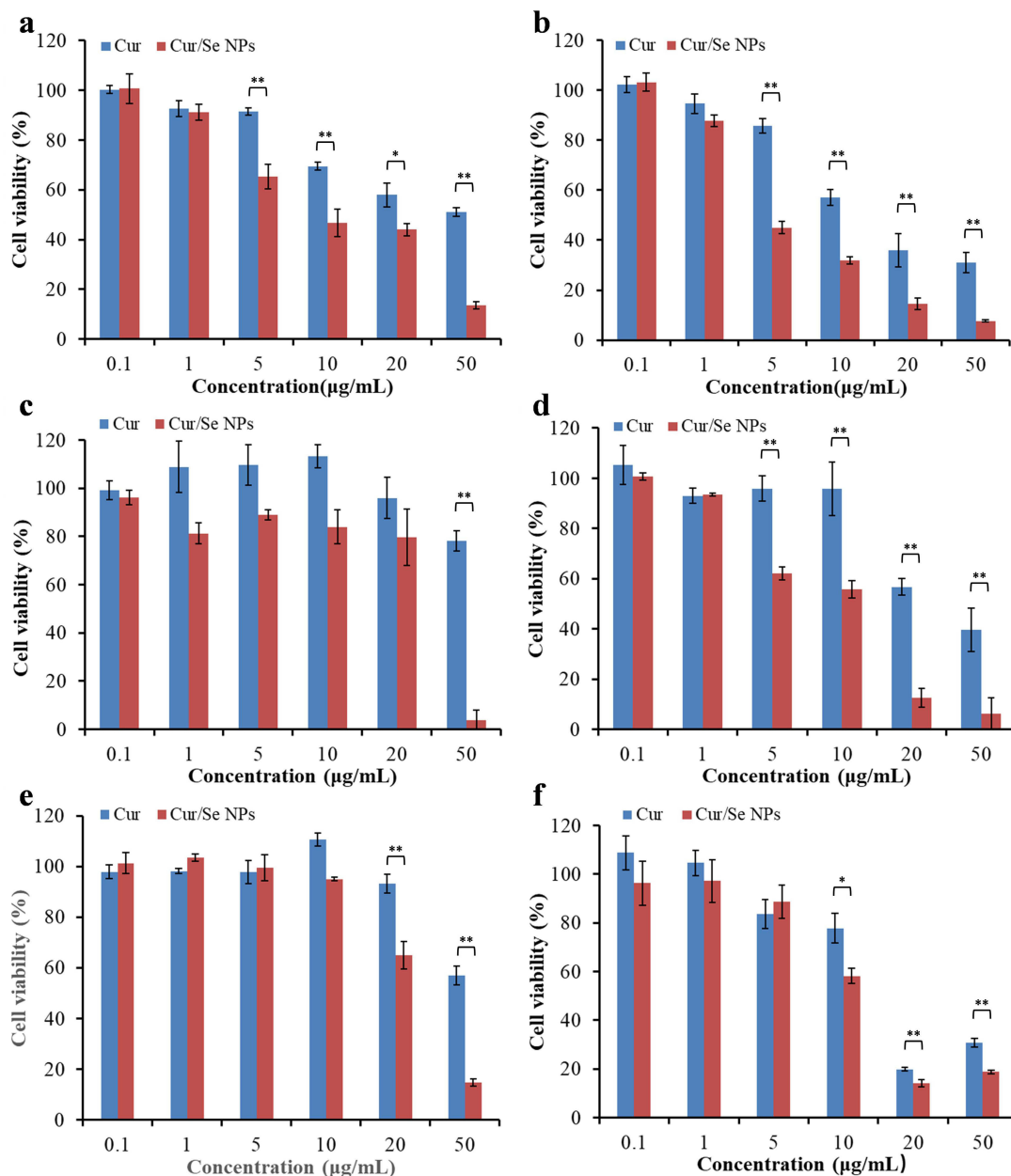
Figure 3 Cytotoxicity of Cur and Cur/Se nanoparticles to HeLa tumour cells at (**a**) 24 h and (**b**) 48 h, as detected by the MTT assay. Cytotoxicity of Cur and Cur/Se nanoparticles to S180 tumour cells at (**c**) 24 h and (**d**) 48 h, as detected by the CCK8 assay. Cytotoxicity of Cur and Cur/Se nanoparticles to L02 cells at (**e**) 24 h and (**f**) 48 h, as detected by the MTT assay. The results are expressed as the means ± SDs (n = 3). **P < 0.01. *P < 0.05.

ROS Level

The ROS levels of the HeLa cells after Cur and Cur/Se nanoparticle treatment are shown in Figure 4c. At a concentration of 2 μg/mL, the relative fluorescence intensity of the Cur group was 0.46 ± 0.01 times that of the control. However, Cur/Se nanoparticle treatment significantly increased the relative fluorescence intensity of DCF to 5.29 ± 0.75 times that of the control. As the curcumin concentration increased to 5 μg/mL, Cur and Cur/Se nanoparticles increased the relative fluorescence intensity of DCF to 2.15 ± 0.26 and 7.69 ± 0.31 times that of the control, respectively. The results showed that Cur could decrease the intracellular ROS level at low concentrations while increasing the intracellular ROS level at high concentrations. Compared with Cur, the Cur/Se nanoparticles significantly improved the ROS level in a concentration-dependent manner. High ROS levels are beneficial for the treatment of tumours.
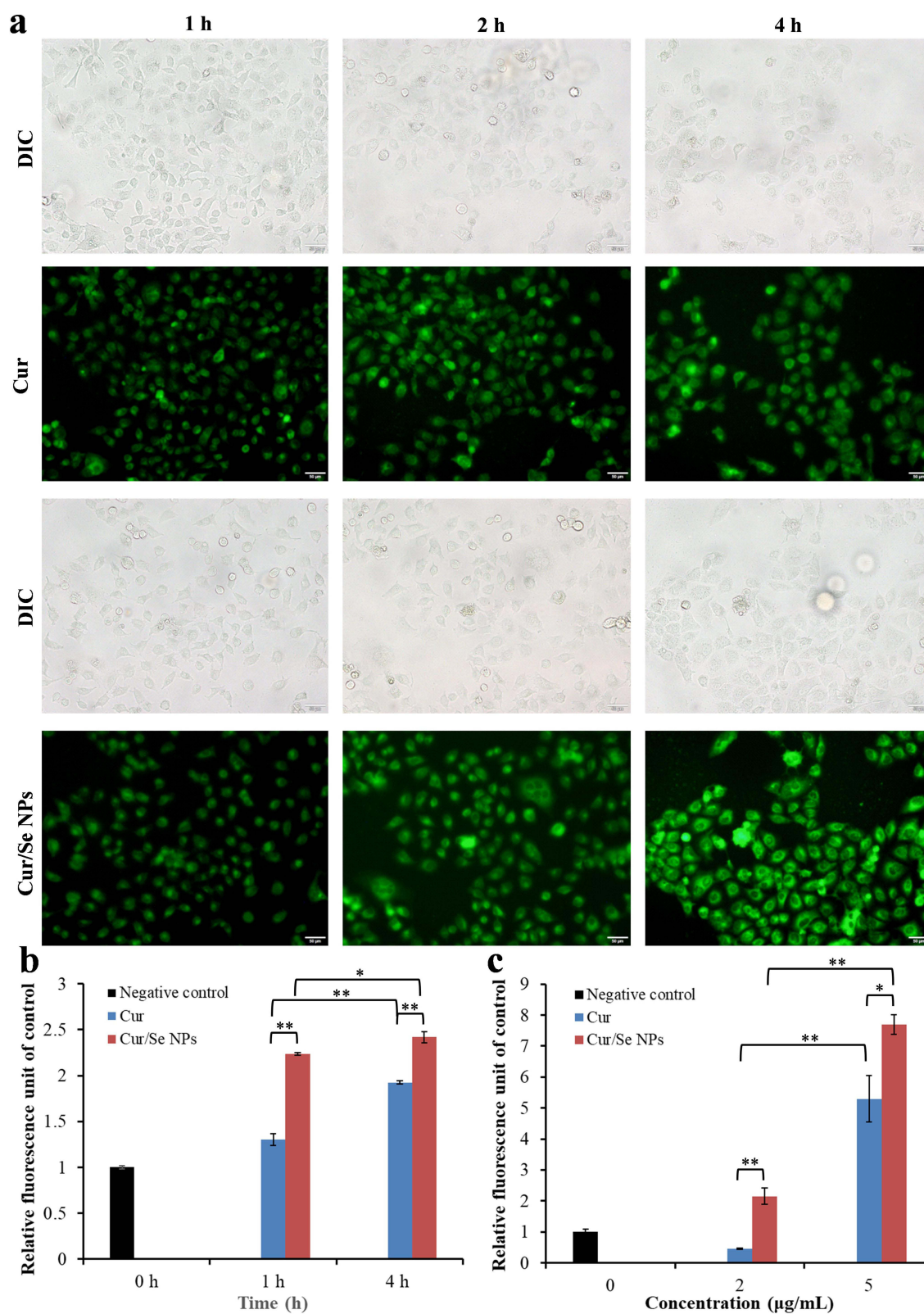
Figure 4 (**a**) Intracellular fluorescence microscopy images of HeLa tumour cells treated with Cur and Cur/Se nanoparticles detected by fluorescence microscopy. The scale bar is 50 μm. (**b**) Fluorescence intensity of HeLa tumour cells treated with Cur and Cur/Se nanoparticles as determined by flow cytometry. (**c**) DCF fluorescence intensity of HeLa tumour cells treated with Cur and Cur/Se nanoparticles was detected by flow cytometry. The results are expressed as the means ± SDs (n = 3). **P < 0.01. *P < 0.05.

In vitro Antibacterial Effect

The in vitro antimicrobial activity was investigated (Figure S1). *Escherichia coli* is a Gram-negative bacterium. The results showed that Cur could not inhibit the growth of *Escherichia coli* (Figure S1a). At the highest concentration of 100 μg/mL, free Cur treated *Escherichia coli* showed a viability of 85.8% ± 5.6%. However, the Cur/Se nanoparticles showed a significant stronger inhibition of *Escherichia coli*. At 25 μg/mL of Cur/Se nanoparticles, the viability of *Escherichia coli* decreased to less than 50%. And the Cur/Se nanoparticles showed concentration dependent antibacterial activity. *Staphylococcus aureus* is a Gram-positive bacterium. The results showed that the Cur/Se nanoparticles had a stronger inhibition of *Staphylococcus aureus* (Figure S1b). As the concentration of free Cur increased to 50 μg/mL, the viability of *Staphylococcus aureus* was as high as 53.9% ± 0.2%. While with the same treatment of Cur/Se nanoparticles, the viability of *Staphylococcus aureus* significantly decreased to 24.1% ± 5.8%. And at 5 μg/mL of Cur/Se nanoparticles, the viability of *Staphylococcus aureus* was 51.1% ± 4.8%. The results showed that the Cur/Se nanoparticles showed greater activity against harmful *Escherichia coli* and *Staphylococcus aureus* compared with Cur in vitro.

In vivo Antitumour Activity

The antitumour effects of free Cur and the Cur/Se nanoparticles are shown in Figure 5. The growth curves of the tumour volume revealed that the growth rate of the tumours treated with free Cur was similar to that of the tumours treated with water (Figure 5a). From Day 6, the mean tumour volume in the Cur group was slightly smaller than that in the control group, and there was no significant difference in the results. The tumour volume in the Cur/Se nanoparticle treatment group was significantly smaller than that in the control and Cur groups, indicating a significant inhibition of tumour growth (**$p < 0.01$). There was no significant difference in body weight among the groups (Figure 5b), and the survival rate of the mice in each group was 100% during the treatment. After 10 days of treatment, the S180-bearing mice were killed, and the tumours were removed and weighed (Figure 5c). The mean tumour weight was 2.00 g in the control group, 1.60 g in the curcumin group, and 0.91 g in the nanoparticle group (Figure 5d). Compared with the free curcumin-treated group, the Cur/Se nanoparticle-treated group presented the smallest tumour weight (*$p < 0.05$ compared with the free curcumin-treated group and **$p < 0.01$ compared with the control group). The tumour inhibitory rate of free curcumin was 19.76%, and that of the Cur/Se nanoparticles was 54.33%. The HE staining results are shown in Figure 5e. The cells of the heart, liver, spleen, lung and kidney in each group were arranged neatly. There was no inflammatory cell infiltration, indicating that there was no obvious tissue damage. The results showed that oral curcumin and nanoparticle therapy had good biocompatibility.

Analysis of the Gut Microbiota

An increasing number of studies have shown that the gut microbiota is closely related to tumour treatment. By analysing the faecal microbiota of mice in different treatment groups, the regulatory effect of Cur/Se nanoparticles on the gut microbiota was explored. The 16S rRNA gene sequencing results revealed that the α-diversity of the gut microbiota was significantly greater in response to Cur/Se nanoparticle treatment than in response to Cur treatment and that the richness and diversity of the microbial community were significantly greater (Figure 6a). S180 tumour-bearing mice treated with Cur or Cur/Se nanoparticles presented significant changes in community composition according to principal coordinate analysis (PCoA) of β diversity (Figure 6b). Community histogram analysis revealed the relative abundance of the gut microbiota at the family level (Figure 6c), and community heatmap analysis revealed the relative abundance of the top 50 microbiota at the genus level (Figure 6d). Compared with the control treatment, Cur and Cur/Se nanoparticle treatment significantly reduced the relative abundance of harmful bacteria such as *Rikenellaceae_RC9_gut_group, Enterorhabdus* and *Bilophila* at the genus level (Figure 6e). The relative abundance of beneficial *Lachnospiraceae_UCG-006* increased after treatment with Cur and Cur/Se nanoparticles (Figure 6f). Moreover, compared with Cur treatment, Cur/Se nanoparticle treatment significantly improved the relative abundance of beneficial *Limosilactobacillus* (Figure 6f).

Discussion

ROS are the main molecules produced by oxidative stress in the body and are closely related to the occurrence, development, and apoptosis of tumours.[22] In normal cells, the oxidation and antioxidant systems are relatively balanced.
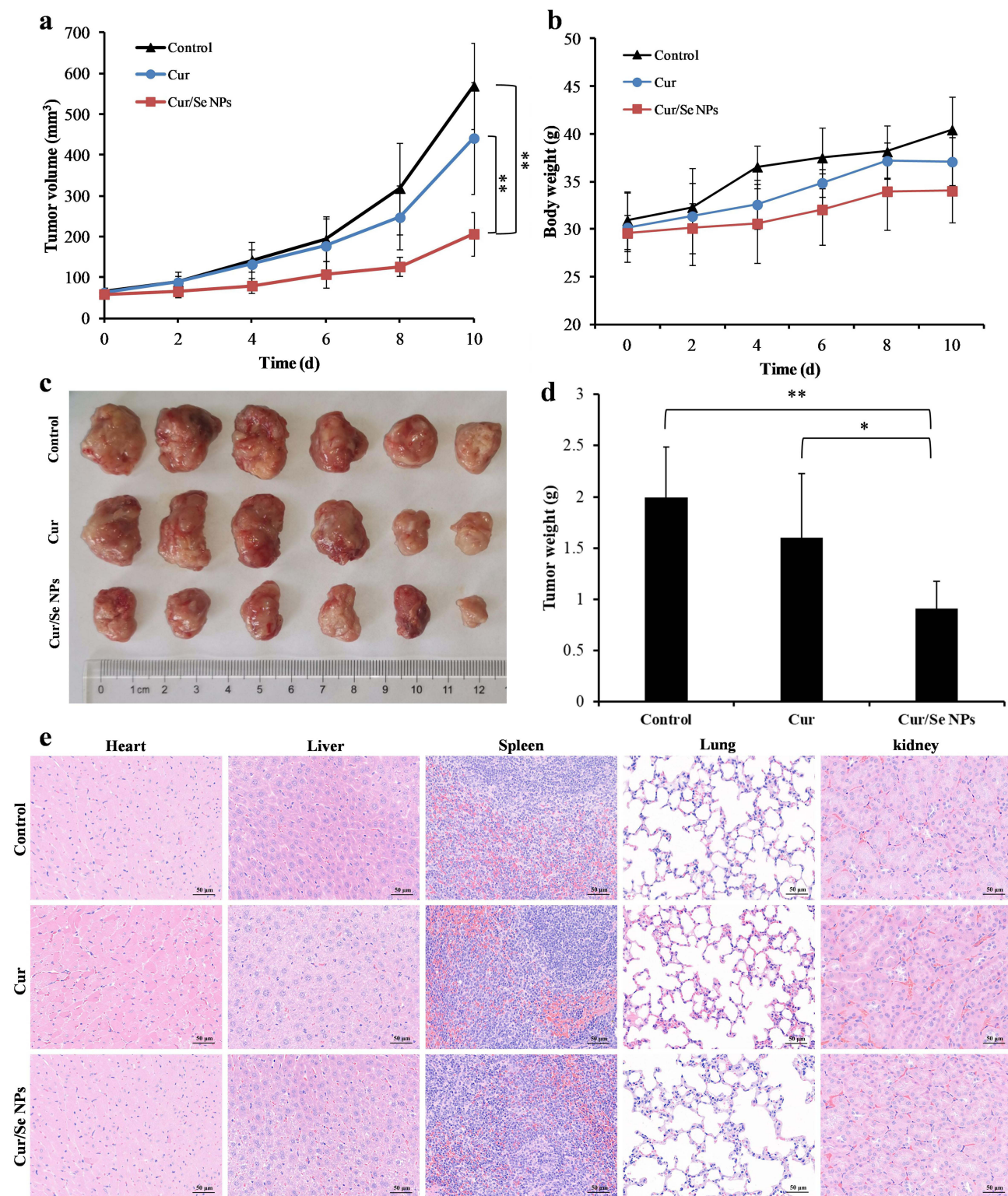
Figure 5 Anti-S180 tumour study in vivo. (**a**) S180 tumour growth curves. (**b**) Body weight curves. (**c**) Photograph of excised tumours. (**d**) Excised tumour weights on Day 10. (**e**) HE staining of the organs. The results are expressed as the means ± SDs (n = 6). *P < 0.05. **P < 0.01.

However, the level of ROS in tumour cells is greater than that in normal cells. Therefore, tumour cells are in a state of oxidative stress and are more sensitive to ROS than normal cells.[23] Thus, ROS are considered tumour-specific targets for the rational design of anticancer agents. Among the redox regulatory agents, curcumin and selenium compounds have received extensive attention because of their good chemotherapy potential.
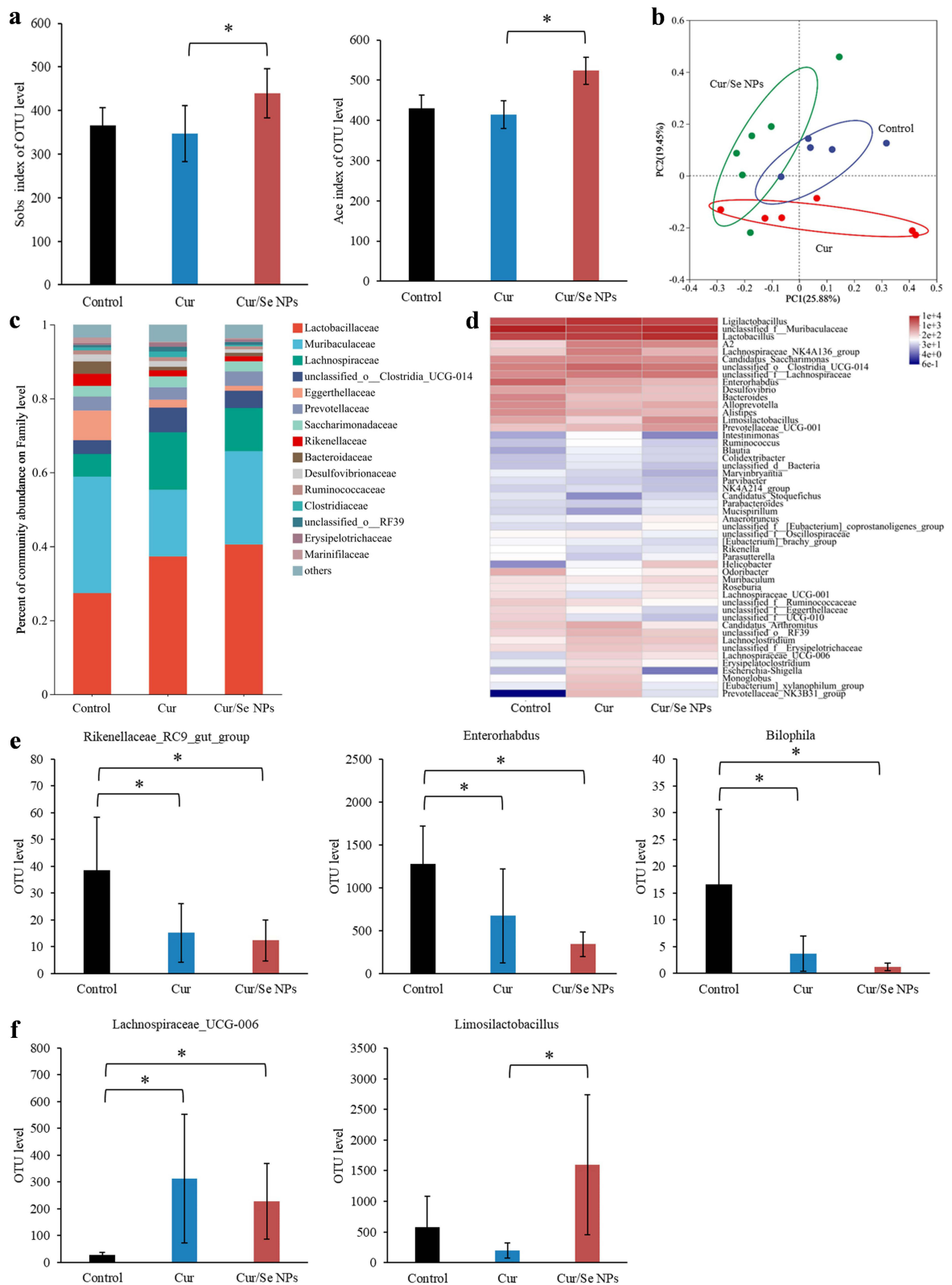
Figure 6 Regulation of the gut microbiota. (**a**) Microbial α diversity in terms of the Sobs and Ace indices at the operational taxonomic unit (OTU) level. (**b**) Microbial β diversity illustrated by a PCoA plot. (**c**) Relative abundance of the gut microbiota at the family level. (**d**) Heatmap of the relative abundance of the gut microbiota at the genus level. (**e**) Relative abundance of harmful *Rikenellaceae_RC9_gut_group, Enterorhabdus* and *Bilophila*. (**f**) Relative abundances of beneficial *Lachnospiraceae_UCG-006* and *Limosilactobacillus*. The results are expressed as the means ± SDs (n = 6). *P < 0.05.

However, curcumin is a hydrophobic drug with poor water solubility and limited permeability in the gastrointestinal mucosa.[24] In addition, curcumin can be quickly eliminated from the system because of its strong gut-liver metabolism in vivo.[24] Therefore, the poor bioavailability of curcumin has limited its application. Nanopreparations of curcumin provide strategies to improve the bioavailability of curcumin.[25]

Selenium nanoparticles are an effective form of selenium with high activity and low toxicity. Using plant extracts to synthesize selenium nanoparticles is a green and environmentally friendly method. Plant-based selenium nanoparticles are prepared by reducing selenium ions with plant extracts, such as *Rosmarinus officinalis*,[26] peppers,[27] and *Punica granatum*,[28] among others. These natural plant extracts can not only reduce selenium ions into selenium nanoparticles but also play a stable dispersion role by attaching or wrapping the nanoparticles to prevent their agglomeration.

Therefore, we designed a simple method to prepare Cur/Se nanoparticles by reducing sodium selenite with curcumin in one step. During the preparation process, nanoparticles with excellent water solubility could be obtained by adding the extra stabilizer Tween 80. Tween 80 is a widely used surfactant with good biocompatibility.[29] Tween 80 can be coated on the surface of Cur/Se nanoparticles, thereby improving their dispersibility in water. The classic method for preparing curcumin-loaded selenium nanoparticles involves two steps. Selenium nanoparticles were prepared first, and curcumin was then loaded onto the selenium nanoparticles.[30] Compared with the reported curcumin-loaded selenium nanoparticles, our method is simpler and more practical. In contrast, the concentration of curcumin in the nanoparticles obtained in this study was more than 200-fold greater than that of selenium.

The characterization of the Cur/Se nanoparticles revealed the same UV absorption as that of curcumin. The FTIR spectra also implied that the Cur/Se nanoparticles retained their active functional groups, such as phenolic hydroxyl, β-diketone, and carbonyl groups. Therefore, the functional properties of the Cur/Se nanoparticles were not affected. Both curcumin and nanoselenium have the ability to scavenge free radicals.[31,32] Under experimental conditions with abundant free radicals, the Cur/Se nanoparticles exhibited excellent antioxidant activity compared with that of curcumin. The cytotoxicity results confirmed the excellent antitumour activity of the Cur/Se nanoparticles in vitro (Scheme 2). The results of the cellular uptake experiments revealed that the Cur/Se nanoparticles could deliver more curcumin into the HeLa tumour cells. The Cur/Se nanoparticles induced more ROS production in tumour cells than free Cur at the same concentration. High-dose curcumin and selenium compounds are oxidants capable of inducing the production of ROS in tumour cells, thereby exerting their potential anticancer effects.[33,34] The combination of curcumin and selenium nanoparticles enhances the antitumour activity of Cur/Se nanoparticles in vitro. For normal L02 cells, the IC_{50} values of Cur and Cur/Se nanoparticles were similar at 48 h, with values of 10.5 μg/mL and 11.2 μg/mL, respectively. For 10 consecutive days of treatment for S180 tumours in vivo, Cur and Cur/Se nanoparticle solutions were orally administered at a dosage of 10 mg/kg per day. After treatment, HE staining of mouse organs revealed no obvious tissue damage. The
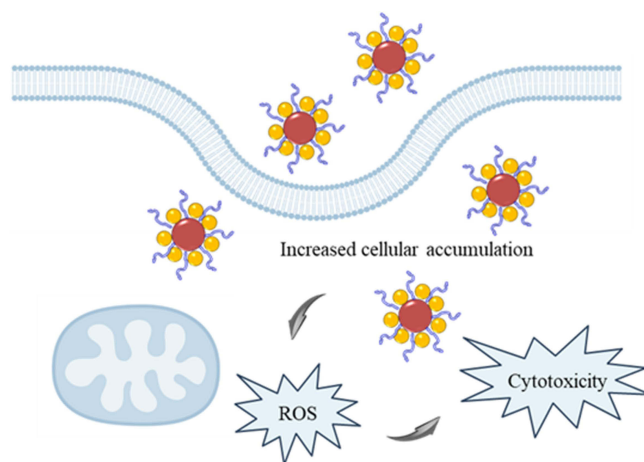
Scheme 2 Schematic illustration of the antitumour activity of Cur/Se nanoparticles in vitro. The Cur/Se nanoparticles could deliver more curcumin into the tumour cells and induce high ROS production, thereby exerting potential antitumour effects.

treatment scheme in this study was relatively safe. The rapid release of Cur and Cur/Se nanoparticles under acidic conditions facilitates the ability of these agents to exert their effects in the acidic tumour environment.[35]

The gut microbiota is a large and complex ecosystem that is considered a potential human organ. The gut microbiota can regulate the immune and metabolic functions of the body, thereby affecting the progression and treatment of various types of cancer. In recent years, the role of the gut microbiota in the development and treatment of tumours has become a popular research area. The gut microbiota has been reported to play an important role in the treatment of tumours via chemotherapy and immunotherapy.[36,37] In this study, Cur/Se nanoparticles were constructed as a gut microbiota-regulating system. Both curcumin and Cur/Se nanoparticles significantly increased the richness and diversity of the microbial community. *Rikenellaceae_RC9_gut_group* has been reported to be positively correlated with cancer-promoting metabolites.[38] *Enterorhabdus*, a harmful bacterium, is reported to be increased in an osteosarcoma mouse model.[39] *Bilophila* can produce genotoxic hydrogen sulfide, which promotes the development of tumours.[40] This study revealed that Cur and Cur/Se nanoparticle treatment inhibited these three harmful bacteria. *Lachnospiraceae_UCG-006* is positively correlated with the activities of antioxidant enzymes.[41] Both curcumin and Cur/Se nanoparticles possess good antioxidant activity and therefore significantly improve the level of *Lachnospiraceae_UCG-006*. *Lachnospira_UCG-006* is a positive short-chain fatty acid-producing bacteria.[42] Moreover, it has been reported that *Lachnospiraceae_UCG-006* is also positively correlated with CD8+ T cells.[43] *Lactobacillus* can produce exopolysaccharides that help probiotics strengthen the immune system and suppress pathogenic bacteria.[44] The significant increase in *Lactobacillus* after Cur/Se nanoparticle treatment improved the antitumour activity. Therefore, the Cur/Se nanoparticles could regulate the gut microbiota by reducing harmful bacteria and increasing beneficial bacteria, thus exerting good antitumour effects.

However, the formation mechanism of Cur/Se nanoparticles needs further exploration. The selenium content in Cur/Se nanoparticles is relatively low, and further optimization of the preparation method is needed to obtain nanoparticles with better activities. In the future, we will study how to improve the tumour targeting ability of Cur/Se nanoparticles to reduce their toxicity to normal cells.

Conclusion

This study provides a simple and green method to prepare Cur/Se nanoparticles in one step. Curcumin was used as a reducing and capping agent in the preparation of the nanoparticles. The Cur/Se nanoparticles showed excellent water dispersibility when Tween 80 was used as the stabilizer. The Cur/Se nanoparticles presented significantly higher DPPH and ABTS radical scavenging rates than did the same concentration of free curcumin. The Cur/Se nanoparticles delivered significantly more curcumin into the HeLa tumour cells and induced greater ROS production. Therefore, the Cur/Se nanoparticles had significant cytotoxicity. The Cur/Se nanoparticles improved the antitumour effect by regulating the gut microbiota in vivo.

Ethics Statement

The animal experiments were approved by the Animal Ethics Committee of Shandong University of Technology (the approval date was 17/11/2021, and the approval certification number of the study was YLX20211101). The study was conducted in accordance with the local legislation and institutional requirements.

Acknowledgments

Disclosure

The authors report no conflicts of interest in this work.

References

1. Yachida S, Mizutani S, Shiroma H, et al. Metagenomic and metabolomic analyses reveal distinct stage-specific phenotypes of the gut microbiota in colorectal cancer. *Nat Med*. 2019;25(6):968–976. doi:10.1038/s41591-019-0458-7

2. Plaza-Díaz J, Álvarez-Mercado AI, Ruiz-Marín CM, et al. Association of breast and gut microbiota dysbiosis and the risk of breast cancer: a case-control clinical study. *BMC Cancer*. 2019;19(1):495. doi:10.1186/s12885-019-5660-y

3. Behary J, Amorim N, Jiang XT, et al. Gut microbiota impact on the peripheral immune response in non-alcoholic fatty liver disease related hepatocellular carcinoma. *Nat Commun*. 2021;12(1):187. doi:10.1038/s41467-020-20422-7

4. Di Modica M, Gargari G, Regondi V, et al. Gut microbiota condition the therapeutic efficacy of trastuzumab in HER2-positive breast cancer. *Cancer Res*. 2021;81(8):2195–2206. doi:10.1158/0008-5472.Can-20-1659

5. Wang M, Huang Y, Xin M, et al. The impact of microbially modified metabolites associated with obesity and bariatric surgery on antitumor immunity. *Front Immunol*. 2023;14:1156471. doi:10.3389/fimmu.2023.1156471

6. Alexander JL, Wilson ID, Teare J, Marchesi JR, Nicholson JK, Kinross JM. Gut microbiota modulation of chemotherapy efficacy and toxicity. *Nat Rev Gastroenterol Hepatol*. 2017;14(6):356–365. doi:10.1038/nrgastro.2017.20

7. Wu MF, Huang YH, Chiu LY, Cherng SH, Sheu GT, Yang TY. Curcumin induces apoptosis of chemoresistant lung cancer cells via ROS-regulated p38 MAPK phosphorylation. *Int J Mol Sci*. 2022;23(15):8248. doi:10.3390/ijms23158248

8. Mortezaee K, Salehi E, Mirtavoos-Mahyari H, et al. Mechanisms of apoptosis modulation by curcumin: implications for cancer therapy. *J Cell Physiol*. 2019;234(8):12537–12550. doi:10.1002/jcp.28122

9. Peterson CT, Vaughn AR, Sharma V, et al. Effects of turmeric and curcumin dietary supplementation on human gut microbiota: a double-blind, randomized, placebo-controlled pilot study. *J Evid Based Integr Med*. 2018;23:2515690x18790725. doi:10.1177/2515690x18790725

10. McFadden RM, Larmonier CB, Shehab KW, et al. The role of curcumin in modulating colonic microbiota during colitis and colon cancer prevention. *Inflamm Bowel Dis*. 2015;21(11):2483–2494. doi:10.1097/mib.0000000000000522

11. Sheng L, Wei Y, Pi C, et al. Preparation and evaluation of curcumin derivatives nanoemulsion based on turmeric extract and its antidepressant effect. *Int J Nanomed*. 2023;18:7965–7983. doi:10.2147/ijn.S430769

12. Zarreen Simnani F, Singh D, Patel P, et al. Nanocarrier vaccine therapeutics for global infectious and chronic diseases. *Mater Today*. 2023;66:371–408. doi:10.1016/j.mattod.2023.04.008

13. Sinha A, Simnani FZ, Singh D, et al. The translational paradigm of nanobiomaterials: biological chemistry to modern applications. *Mater Today Bio*. 2022;17:100463. doi:10.1016/j.mtbio.2022.100463

14. Yan Y, Chen Y, Liu Z, et al. Brain delivery of curcumin through low-intensity ultrasound-induced blood-brain barrier opening via lipid-PLGA nanobubbles. *Int J Nanomed*. 2021;16:7433–7447. doi:10.2147/ijn.S327737

15. Zhang B, Yan J, Jin Y, Yang Y, Zhao X. Curcumin-shellac nanoparticle-loaded GelMA/SilMA hydrogel for colorectal cancer therapy. *Eur J Pharm Biopharm*. 2024;202:114409. doi:10.1016/j.ejpb.2024.114409

16. Li L, Liu Z, Quan J, Sun J, Lu J, Zhao G. Dietary nano-selenium alleviates heat stress-induced intestinal damage through affecting intestinal antioxidant capacity and microbiota in rainbow trout (Oncorhynchus mykiss). *Fish Shellfish Immunol*. 2023;133:108537. doi:10.1016/j.fsi.2023.108537

17. Yu Y, Zhang X, Qiu L. The anti-tumor efficacy of curcumin when delivered by size/charge-changing multistage polymeric micelles based on amphiphilic poly(β-amino ester) derivates. *Biomaterials*. 2014;35(10):3467–3479. doi:10.1016/j.biomaterials.2013.12.096

18. Xie X, Li Y, Zhao D, et al. Oral administration of natural polyphenol-loaded natural polysaccharide-cloaked lipidic nanocarriers to improve efficacy against small-cell lung cancer. *Nanomedicine*. 2020;29:102261. doi:10.1016/j.nano.2020.102261

19. Patil S, Choudhary B, Rathore A, Roy K, Mahadik K. Enhanced oral bioavailability and anticancer activity of novel curcumin loaded mixed micelles in human lung cancer cells. *Phytomedicine*. 2015;22(12):1103–1111. doi:10.1016/j.phymed.2015.08.006

20. Niu F, Hu D, Gu F, et al. Preparation of ultra-long stable ovalbumin/sodium carboxymethylcellulose nanoparticle and loading properties of curcumin. *Carbohydr Polym*. 2021;271:118451. doi:10.1016/j.carbpol.2021.118451

21. Xiang G, Sun H, Chen Y, et al. Antioxidant and hypoglycemic activity of tea polysaccharides with different degrees of fermentation. *Int J Biol Macromol*. 2023;228:224–233. doi:10.1016/j.ijbiomac.2022.12.114

22. Cheung EC, Vousden KH. The role of ROS in tumour development and progression. *Nat Rev Cancer*. 2022;22(5):280–297. doi:10.1038/s41568-021-00435-0

23. Liu Q, Ding X, Xu X, et al. Tumor-targeted hyaluronic acid-based oxidative stress nanoamplifier with ROS generation and GSH depletion for antitumor therapy. *Int J Biol Macromol*. 2022;207:771–783. doi:10.1016/j.ijbiomac.2022.03.139

24. Hegde M, Girisa S, BharathwajChetty B, Vishwa R, Kunnumakkara AB. Curcumin formulations for better bioavailability: what we learned from clinical trials thus far? *ACS omega*. 2023;8(12):10713–10746. doi:10.1021/acsomega.2c07326

25. Ipar VS, Dsouza A, Devarajan PV. Enhancing curcumin oral bioavailability through nanoformulations. *Eur J Drug Metab Pharmacokinet*. 2019;44 (4):459–480. doi:10.1007/s13318-019-00545-z

26. Adibian F, Ghaderi RS, Sabouri Z, et al. Green synthesis of selenium nanoparticles using Rosmarinus officinalis and investigated their antimicrobial activity. *Biometals*. 2022;35(1):147–158. doi:10.1007/s10534-021-00356-3

27. Shah V, Medina-Cruz D, Vernet-Crua A, et al. Pepper-mediated green synthesis of selenium and tellurium nanoparticles with antibacterial and anticancer potential. *J Funct Biomater*. 2022;14(1):24. doi:10.3390/jfb14010024

28. Shnoudeh AJ, Qadumii L, Zihlif M, et al. Green synthesis of gold, iron and selenium nanoparticles using phytoconstituents: preliminary evaluation of antioxidant and biocompatibility potential. *Molecules*. 2022;27(4):1334. doi:10.3390/molecules27041334

29. Roacho-Pérez JA, Ruiz-Hernandez FG, Chapa-Gonzalez C, et al. Magnetite nanoparticles coated with PEG 3350-Tween 80: in vitro characterization using primary cell cultures. *Polymers*. 2020;12(2):300. doi:10.3390/polym12020300

30. Yu S, Wang Y, Zhang W, Zhang Y, Wang J. PH-assisted surface functionalization of selenium nanoparticles with curcumin to achieve enhanced cancer chemopreventive activity. *RSC Adv*. 2016;6(76):72213–72223. doi:10.1039/c6ra13291j

31. Purushothaman A, Teena Rose KS, Jacob JM, Varatharaj R, Shashikala K, Janardanan D. Curcumin analogues with improved antioxidant properties: a theoretical exploration. *Food Chem*. 2022;373(Pt B):131499. doi:10.1016/j.foodchem.2021.131499

32. Bjørklund G, Shanaida M, Lysiuk R, et al. Selenium: an antioxidant with a critical role in anti-aging. *Molecules*. 2022;27(19):6613. doi:10.3390/molecules27196613

33. Li G, Fang S, Shao X, et al. Curcumin reverses NNMT-induced 5-fluorouracil resistance via increasing ROS and cell cycle arrest in colorectal cancer cells. *Biomolecules*. 2021;11(9):1295. doi:10.3390/biom11091295

34. Sonkusre P, Cameotra SS. Biogenic selenium nanoparticles induce ROS-mediated necroptosis in PC-3 cancer cells through TNF activation. *J Nanobiotechnology*. 2017;15(1):43. doi:10.1186/s12951-017-0276-3

35. Xu B, Zhou W, Cheng L, et al. Novel polymeric hybrid nanocarrier for curcumin and survivin shRNA co-delivery augments tumor penetration and promotes synergistic tumor suppression. *Front Chem*. 2020;8:762. doi:10.3389/fchem.2020.00762

36. Vétizou M, Pitt JM, Daillère R, et al. Anticancer immunotherapy by CTLA-4 blockade relies on the gut microbiota. *Science*. 2015;350 (6264):1079–1084. doi:10.1126/science.aad1329

37. Zheng DW, Dong X, Pan P, et al. Phage-guided modulation of the gut microbiota of mouse models of colorectal cancer augments their responses to chemotherapy. *Nat Biomed Eng*. 2019;3(9):717–728. doi:10.1038/s41551-019-0423-2

38. Yang Y, Dai D, Jin W, et al. Microbiota and metabolites alterations in proximal and distal gastric cancer patients. *J Transl Med*. 2022;20(1):439. doi:10.1186/s12967-022-03650-x

39. Tian Z, Qiao X, Wang Z, et al. Cisplatin and doxorubicin chemotherapy alters gut microbiota in a murine osteosarcoma model. *Aging*. 2024;16 (2):1336–1351. doi:10.18632/aging.205428

40. Dahmus JD, Kotler DL, Kastenberg DM, Kistler CA. The gut microbiome and colorectal cancer: a review of bacterial pathogenesis. *J Gastrointest Oncol*. 2018;9(4):769–777. doi:10.21037/jgo.2018.04.07

41. Yang L, Wang Y, Zheng G, Li Z, Mei J. Resveratrol-loaded selenium/chitosan nano-flowers alleviate glucolipid metabolism disorder-associated cognitive impairment in Alzheimer's disease. *Int J Biol Macromol*. 2023;239:124316. doi:10.1016/j.ijbiomac.2023.124316

42. Guo W, Xiang Q, Mao B, et al. Protective effects of microbiome-derived inosine on lipopolysaccharide-induced acute liver damage and inflammation in mice via mediating the TLR4/NF-κB pathway. *J Agric Food Chem*. 2021;69(27):7619–7628. doi:10.1021/acs.jafc.1c01781

43. Yao Y, Feng S, Li X, et al. Litchi procyanidins inhibit colon cancer proliferation and metastasis by triggering gut-lung axis immunotherapy. *Cell Death Dis*. 2023;14(2):109. doi:10.1038/s41419-022-05482-5

44. Ksiezarek M, Grosso F, Ribeiro TG, Peixe L. Genomic diversity of genus Limosilactobacillus. *Microb Genom*. 2022;8(7):mgen000847. doi:10.1099/mgen.0.000847